

# Spectroscopic survey of emission-line stars – I. B[e] stars<sup>★</sup>

A. Aret,<sup>1†</sup> M. Kraus<sup>1,2</sup> and M. Šlechta<sup>2</sup>

<sup>1</sup>Tartu Observatory, 61602 Tõravere, Tartumaa, Estonia

<sup>2</sup>Astronomický ústav, Akademie věd České republiky, Fričova 298, CZ-25165 Ondřejov, Czech Republic

Accepted 2015 November 20. Received 2015 November 20; in original form 2015 August 11

## ABSTRACT

Emission-line stars are typically surrounded by dense circumstellar material, often in form of rings or disc-like structures. Line emission from forbidden transitions trace a diversity of density and temperature regimes. Of particular interest are the forbidden lines of [O I]  $\lambda\lambda$ 6300, 6364 and [Ca II]  $\lambda\lambda$ 7291, 7324. They arise in complementary, high-density environments, such as the inner-disc regions around B[e] supergiants. To study physical conditions traced by these lines and to investigate how common they are, we initiated a survey of emission-line stars. Here, we focus on a sample of nine B[e] stars in different evolutionary phases. Emission of the [O I] lines is one of the characteristics of B[e] stars. We find that four of the objects display [Ca II] line emission: for the B[e] supergiants V1478 Cyg and 3 Pup, the kinematics obtained from the [O I] and [Ca II] line profiles agrees with a Keplerian rotating disc scenario; the forbidden lines of the compact planetary nebula OY Gem display no kinematical broadening beyond spectral resolution; the luminous blue variable candidate V1429 Aql shows no [O I] lines, but the profile of its [Ca II] lines suggests that the emission originates in its hot, ionized circumbinary disc. As none of the B[e] stars of lower mass displays [Ca II] line emission, we conclude that these lines are more likely observable in massive stars with dense discs, supporting and strengthening the suggestion that their appearance requires high-density environments.

**Key words:** circumstellar matter – stars: emission line, Be – stars: winds, outflows.

## 1 INTRODUCTION

Massive stars ( $>8 M_{\odot}$ ) play a major role in the evolution of their host galaxies. Via their stellar winds, they strongly enrich the interstellar medium with chemically processed material and deposit large amounts of momentum and energy into their surroundings during their entire lifetime, before they end their lives in spectacular supernova explosions. During their evolution, massive stars can pass through short-lived phases of enhanced mass-loss and mass ejections. Well-known groups in such transition phases are the luminous blue variables (LBVs), red supergiants (RSGs), yellow hypergiants (YHG), and B[e] supergiants (B[e]SGs). The ejected material typically accumulates in either shells, rings, or disc-like structures and often veils the central star. Moreover, the conditions within the ejecta, with respect to temperature and density, favour a rich chemistry, including the formation of molecules and condensation of dust particles. Consequently, these stars display rich emission line spectra, facilitating studies of structure and kinematics of the circumstellar material.

Besides the lines from the hydrogen recombination series, forbidden emission lines belong to the prominent features observed from circumstellar environments. The shape and strength of their profiles provide direct access to the structure (density, temperature) and gas dynamics of their formation regions. The lines of [O I]  $\lambda\lambda$ 6300, 6364 and [Ca II]  $\lambda\lambda$ 7291, 7324 have recently proven to trace predominantly high-density gas regions, such as the innermost disc regions of B[e]SGs (Kraus, Borges Fernandes & de Araújo 2007, 2010; Aret et al. 2012). They were also reported from a few young stellar objects (Hamann 1994; Hartigan, Edwards & Pierson 2004), as well as from the dense winds or outflows of YHGs (e.g. Humphreys et al. 2013, 2014). Other forbidden lines, such as [Fe II], [S II], [N II], etc., trace regions of low(er) density but diverse temperatures and deliver complementary information from physically disjoint regions. The permitted lines of the Ca II IR triplet ( $\lambda\lambda$ 8498, 8542, 8662) are observed in a variety of objects, including T Tauri stars (e.g. Hamann & Persson 1992a; Kwan & Fischer 2011), Herbig Ae/Be stars (e.g. Hamann & Persson 1992b), classical Be stars (e.g. Polidan & Peters 1976; Briot 1981; Andriolat, Jaschek & Jaschek 1988, 1990; Jaschek et al. 1988), B[e]SGs (Kraus et al. 2010; Aret et al. 2012), and other, non-supergiant B[e] stars (Borges Fernandes et al. 2001, 2009). These triplet lines are often composite, possessing contributions from both a less dense wind and a dense shell or disc (Aret et al. 2012).

<sup>★</sup> Based on observations collected with the Perek 2-m telescope at Ondřejov Observatory, Czech Republic.

† E-mail: [anna.aret@to.ee](mailto:anna.aret@to.ee)

**Table 1.** Target list. Radial velocities  $V_r$  were derived using all available forbidden emission lines.

Identifier I	Identifier II	HD	$\alpha$ (J2000.0)	$\delta$ (J2000.0)	$V$ (mag)	Class <sup>a</sup>	Sp. type	Ref.	$V_r$ (km s <sup>-1</sup> )
V1478 Cyg	MWC 349A		20 32 45.53	+40 39 36.6	13.0	B[e]SG	B0-B1.5 I	(1)	$-9 \pm 2$
3 Pup	MWC 570	62623	07 43 48.47	-28 57 17.4	3.9	B[e]SG	A2.7 Ib	(2)	$23 \pm 2$
CI Cam	MWC 84		04 19 42.13	+55 59 57.7	11.8	B[e]SG	B0-2 I	(3)	$-51 \pm 2$
V1972 Cyg	MWC 342		20 23 03.61	+39 29 50.1	10.6	B[e]SG cand	B0-2	(4)	$-23 \pm 1$
V1429 Aql	MWC 314		19 21 33.97	+14 52 56.9	9.9	B[e]SG cand	B3 Ibe	(5)	$29 \pm 1$
OY Gem	MWC 162	51585	06 58 30.41	+16 19 26.1	11.2	B[e] cPNe	OBpe	(6)	$54 \pm 1$
V743 Mon	MWC 158	50138	06 51 33.40	-06 57 59.4	6.6	B[e] uncl	B6-7 III-V	(7)	$38 \pm 1$
BD+23 3183	IRAS 17449+2320		17 47 03.28	+23 19 45.4	10.0	B[e] uncl <sup>b</sup>	A0	(8)	$-17 \pm 3$
HD 281192	MWC 728	281192	03 45 14.72	+29 45 03.2	9.8	B[e] uncl <sup>b</sup>	B5 + G8	(9)	$28 \pm 2$

Notes. <sup>a</sup>Classification according to the evolutionary state: B[e]SG (cand) = B[e] supergiant (candidate), B[e] cPNe = compact planetary nebula B[e] star, B[e] uncl = unclassified B[e] star.

<sup>b</sup>Objects were suggested by Miroshnichenko et al. (2007) to be of FS CMA type.

References: (1) Gvaramadze & Menten (2012); (2) Klochkova, Sendzikas & Chentsov (2015); (3) Hynes et al. (2002); (4) Miroshnichenko & Corporon (1999); (5) Carmona et al. (2010); (6) Jaschek et al. (1996); (7) Borges Fernandes et al. (2009); (8) Miroshnichenko et al. (2007); (9) Miroshnichenko et al. (2015).

Interestingly, the lower energy levels, to which the calcium infrared (IR) triplet lines decay, are the upper levels of two forbidden transitions ([Ca II]  $\lambda\lambda 7291, 7324$ ). Therefore, the appearance of the [Ca II] lines could be a suitable tracer for specific temperature and density conditions within the high-density environments of emission-line stars. Pioneering investigations have recently been started by Aret et al. (2012) for the discs of B[e]SGs. In their studies, the authors found that the [Ca II] lines in these objects originate from disc regions close to the star, and the [O I] lines arise from either the same or a slightly lower density region, i.e. from farther out. As the discs of B[e]SGs are typically in Keplerian rotation (see e.g. Kraus et al. 2010, 2013, 2014, 2015; Millour et al. 2011; Cidale et al. 2012; Wheelwright et al. 2012; Muratore et al. 2015), the analysis of the profiles of both the [Ca II] and [O I] lines have been used by Aret et al. (2012) to constrain the kinematics and the inclination angles. These results, combined with the outcome of earlier studies (see Kraus et al. 2005), clearly demonstrate the great potential of the different, complementary sets of forbidden emission lines in determining structure and kinematics of circumstellar gas.

However, the frequency and origin of the [Ca II] lines in stars with circumstellar discs or dense environments is not well studied yet. Also unclear are the proper physical conditions in terms of temperature and density ranges necessary for the excitation of these forbidden lines. Hence, systematic surveys and studies of stars with high-density environments are needed to shed light on a possible link between the appearance of the [Ca II] lines and other prominent disc emission features, such as the [O I] and the Ca II IR triplet lines, and to provide important information on the physical conditions in their formation regions. Therefore, we started a survey of emission-line stars and disc sources in a variety of evolutionary stages, aimed at finding objects that show the strategic [Ca II] and [O I] lines as possible tracers of high-density discs or shells.

One group of stars surrounded by dusty shells, rings or discs, as is evident from their IR excess emission (Allen & Swings 1976), are the B[e] stars (or, more precisely, stars showing the B[e] phenomenon). The optical spectra of these objects typically display strong Balmer line emission, together with emission of low-ionized metals from both permitted and forbidden transitions. These spectral characteristics are seen in stars of diverse evolutionary phases. Lamers et al. (1998) were the first to sort B[e] stars according to their evolutionary stage. They found pre-main-sequence (Herbig Ae/B[e]) stars, as well as evolved objects such as compact

planetary nebulae and B[e]SGs. In addition, several B[e] stars turned out to be symbiotic objects. However, for more than half of the known B[e] stars no appropriate evolutionary stage could be assigned, either because of the lack of proper stellar parameters, such as distance hence luminosity, or because the stars display spectral characteristics in common with more than just one classification. These stars are gathered within the group of unclassified B[e] stars.

## 2 OBSERVATIONS AND DATA REDUCTION

Our sample contains nine Galactic northern B[e] stars of different masses and in different evolutionary stages. In particular, we have three supergiants, two supergiant candidates, one compact planetary nebula, and three B[e] stars with unclear evolutionary state. The objects are listed in Table 1 together with their coordinates,  $V$ -band magnitudes, classification, and spectral types collected from the literature.

The observations were obtained using the Coudé spectrograph attached to the Perek 2-m telescope at Ondřejov Observatory (Šlechta & Škoda 2002). We used the 830.77 lines mm<sup>-1</sup> grating produced by Bausch & Lomb with a SiTe 2030×800 CCD. Spectra were taken in three different wavelength regions: around H  $\alpha$  (6250 to 6760 Å), in the region of the [Ca II]  $\lambda\lambda 7291, 7324$  lines (6990 to 7500 Å), and in the region of the Ca II IR triplet (8470 to 8980 Å). The H  $\alpha$  region also encloses the two [O I]  $\lambda\lambda 6300, 6364$  lines. The spectral resolution achieved in each range is  $R \simeq 13\,000$  in the H  $\alpha$  region,  $R \simeq 15\,000$  in the [Ca II] region, and  $R \simeq 18\,000$  in the Ca II IR triplet region. For wavelength calibration, a comparison spectrum of a ThAr lamp was taken immediately after each exposure. The stability of the wavelength scale was verified by measuring the wavelength centroids of [O I] sky lines. The velocity scale remained stable within 1 km s<sup>-1</sup>.

Spectra in the three different wavelength regions were taken within the same night or, if this was not possible, close in time. Details on the observations and the quality of the spectra are provided in the observing log (Table 2). The data were reduced using standard IRAF<sup>1</sup> tasks, such as bias subtraction, flat-field normalization, and wavelength calibration. To perform telluric corrections in

<sup>1</sup> IRAF is distributed by the National Optical Astronomy Observatories, which are operated by the Association of Universities for Research in Astronomy, Inc., under cooperative agreement with the National Science Foundation.

**Table 2.** Observing log.

Star	H $\alpha$			Ca IR triplet			[Ca II]		
	Date	$T_{\text{exp}}$ (s)	S/N	Date	$T_{\text{exp}}$ (s)	S/N	Date	$T_{\text{exp}}$ (s)	S/N
V1478 Cyg	2012-08-15	3600	25	2012-08-15	3600	35	2012-08-15	3600	35
3 Pup	2011-10-16	400	135	2012-04-07	370	45	2011-10-16	400	150
CI Cam	2011-10-01	3600	60	2011-09-30	3600	40	2011-09-30	3600	50
V1972 Cyg	2011-08-19	3001	80	2012-04-30	3600	60	2011-08-18	3600	100
V1429 Aql	2012-03-24	3600	65	2012-03-24	707	25	2012-03-24	3600	50
OY Gem	2012-03-20	3600	17	2012-03-18	3169	8	2012-03-18	1347	10
V743 Mon	2012-01-31	2700	135	2012-01-31	3600	80	2012-02-03	3600	140
BD+23 3183	2011-08-23	3600	80	2012-08-15	3600	50	2011-08-23	3600	80
HD 281192	2012-08-20	3600	100	2012-08-16	3600	55	2012-08-16	3600	80

all three wavelength regions, telluric standard stars were observed each night. The final spectra were corrected for heliocentric and systemic velocities and normalized. The systemic velocities were obtained from the forbidden lines in our spectra, and the values are included in Table 1.

### 3 RESULTS

Figs 1–3 display the spectral ranges around the forbidden lines of our interest. Shown are the regions of the [O I]  $\lambda\lambda$ 6300, 6364 lines (left) and of the [Ca II]  $\lambda\lambda$ 7291, 7324 lines (right). We grouped the

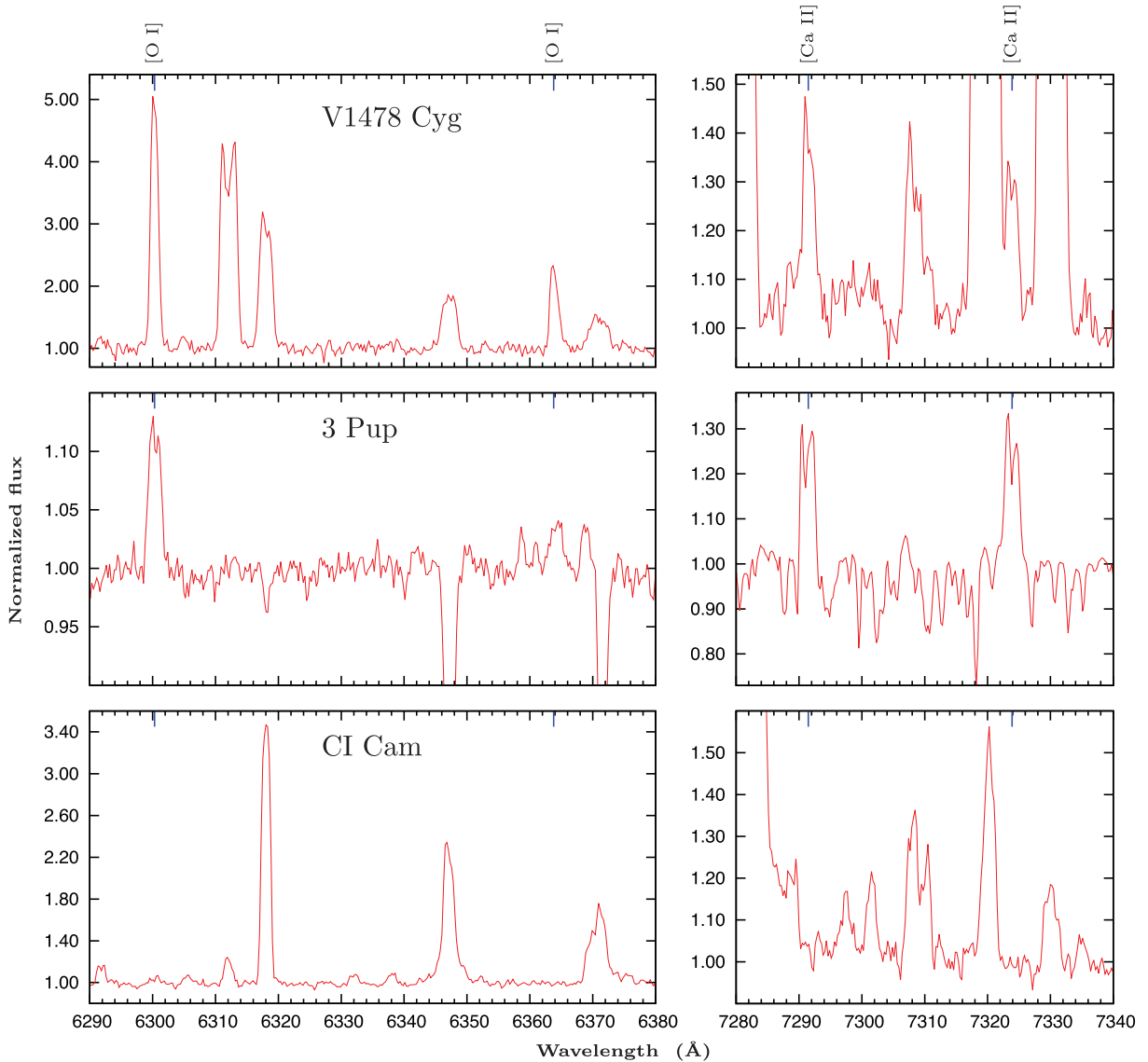


**Figure 1.** Spectral portions of B[e]SG stars covering the strategic forbidden lines of [O I]  $\lambda\lambda$ 6300, 6364 and [Ca II]  $\lambda\lambda$ 7291, 7324. The wavelengths of the lines are marked by ticks. Spectra are corrected for heliocentric and systemic velocities.

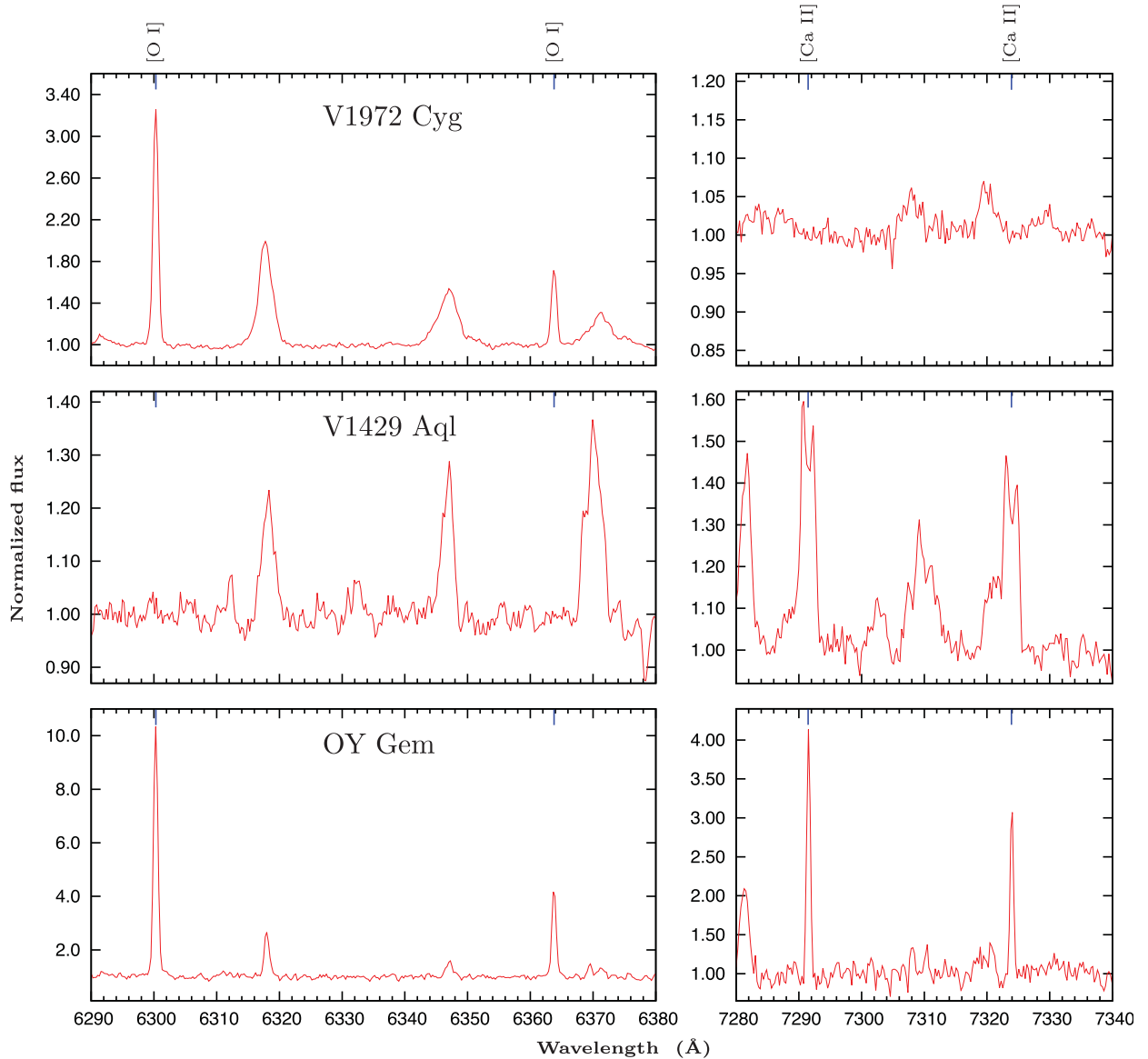


Figure 2. As Fig. 1, but for the two B[e]SG candidates and the compact planetary nebula.

B[e]SGs in Fig. 1, the B[e]SG candidates and the compact planetary nebula in Fig. 2, and the remaining objects in Fig. 3. Maintaining the same order of the stars, we show in Figs 4–6 the  $H\alpha$  line (left) and the  $\text{Ca II}$  IR triplet ( $\lambda\lambda 8498, 8542, 8662$ , right). The latter region also encompasses four hydrogen Paschen (Pa) lines, Pa(16) to Pa(13). Three of them appear in the close vicinity of the  $\text{Ca II}$  triplet lines. In most of our spectra,  $\text{Ca II}$  triplet and Pa lines are blended, hampering a clear identification and classification of their profile shapes. The wavelengths of all these lines are marked in each panel and their identification is given on top of the figures.

Inspection of the spectra reveals that all objects display  $[\text{O I}]$  emission, except CI Cam and, possibly, V1429 Aql. Although V1429 Aql has a weak emission feature in the vicinity of the wavelength of the  $[\text{O I}] \lambda 6300$  line, its radial velocity of only  $\sim 5 \pm 10 \text{ km s}^{-1}$  disagrees with the value measured from other emission lines in that star ( $29 \pm 1 \text{ km s}^{-1}$ , see Table 1). The two objects have further in common that their  $H\alpha$  line is single peaked, while in all other stars  $H\alpha$  is double peaked, with the red peak typically more intense than the blue one.

The  $[\text{Ca II}]$  lines are detected in four objects: V1478 Cyg, 3 Pup, V1429 Aql, and OY Gem. All stars with  $[\text{Ca II}]$  emission also have emission in the  $\text{Ca II}$  IR triplet lines. The reverse is, however, not true, with CI Cam, V1972 Cyg, and V743 Mon as examples. In the latter two stars the triplet lines are strongly blended with broad Pa line emission that dominates the red spectra. In contrast, in 3 Pup and V 1429 Aql the Pa lines are in absorption and weak emission, respectively, while the triplet displays prominent emission lines. Two of the objects, BD+23 3183 and HD 281192, display emission of neither the  $[\text{Ca II}]$  nor the IR triplet lines. Both stars are unclassified regarding their evolutionary phase, but are presumably dwarfs with masses  $< 8 M_{\odot}$  (Miroschnichenko et al. 2007, 2015).

Where appropriate, we measure the width of the lines in velocity units at the continuum level and at half of the maximum value, and for the double-peaked lines also the peak separation. These values, together with a description of the shape of the individual lines, are listed in Table 3 for the forbidden lines of  $[\text{O I}]$  and  $[\text{Ca II}]$ . For  $H\alpha$  and the  $\text{Ca II}$  IR triplet, we only provide details on their profile

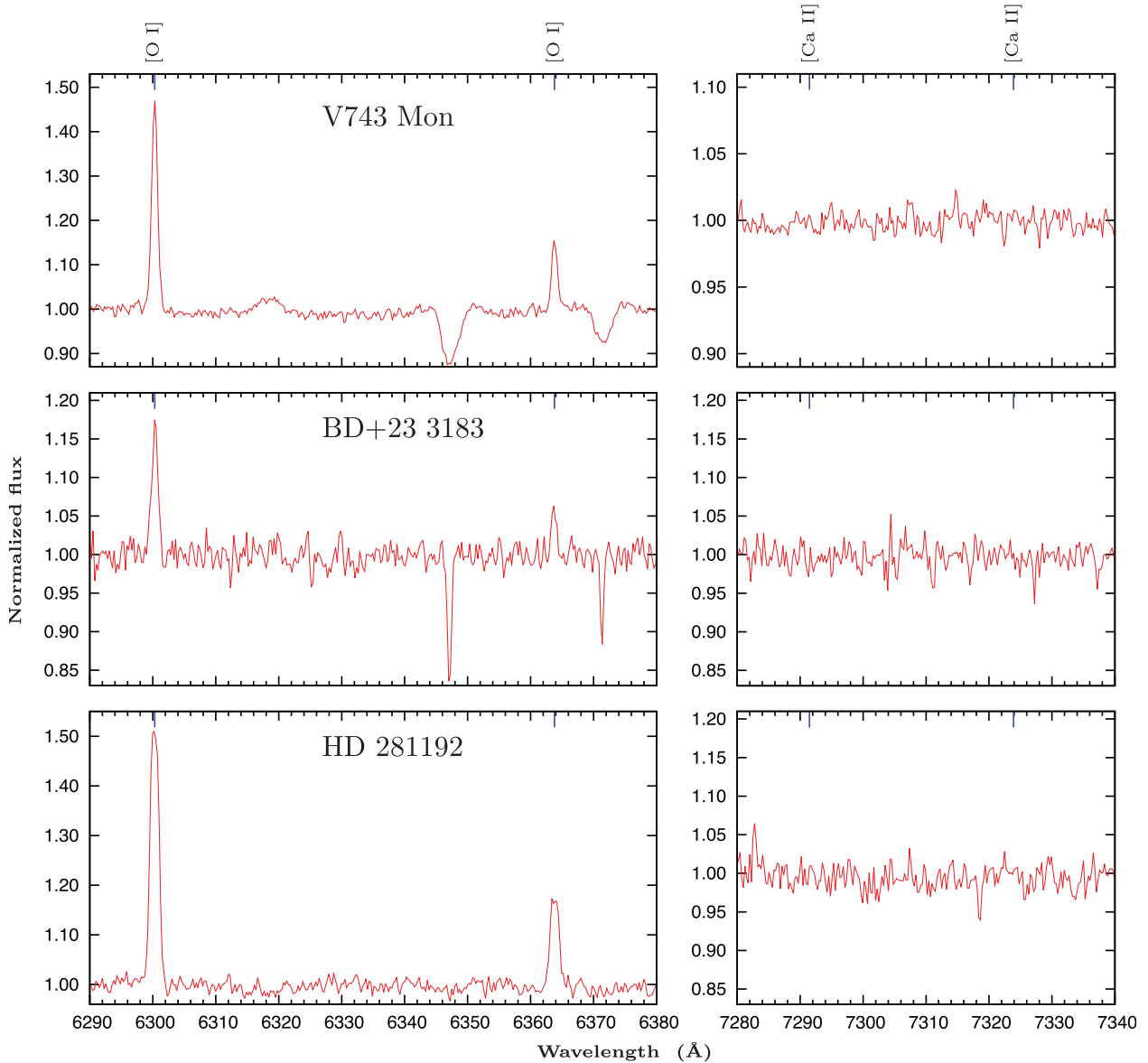


**Figure 3.** As Fig. 1, but for the unclassified B[e] stars.

shape (if resolved) in Table 4. Moreover, stellar parameters were collected from the literature and summarized in Table 5. In this table, we also provide information on the existence of a circumstellar disc and on emission of CO bands, which could mark the inner rim of the molecular disc. We mark the presence of a disc only for those objects with yes, for which a definite proof for the existence is available, either directly from (spectro-)polarimetric or interferometric observations, or indirectly from kinematical analyses of a large number of emission lines. Although a double-peaked  $H\alpha$  line profile is a strong indication for a gas disc, this alone cannot be considered as a proof of a disc-like structure, because such a profile can arise in a variety of configurations of the circumstellar matter, even in a spherically symmetric wind, as shown by Cidale & Ringuet (1993). Hence, stars that were reported so far only as having a double-peaked  $H\alpha$  line profile are marked in the table with uncertain disc presence. In the following, we review each object and discuss the observed spectral appearance in the frame of the characteristics of the circumstellar environment.

### V1478 Cyg = MWC 349A

V1478 Cyg (MWC 349A) is the more massive component of MWC 349. The B component is a B0 III star, located 2.4 arcsec west of the main component, which is a highly reddened ( $A_V \simeq 10$  mag) B0-1.5 I star. Luminosity determinations for the main component range from  $\sim 3 \times 10^4 L_\odot$  (Cohen et al. 1985) to  $(4-8) \times 10^5 L_\odot$  (Gvaramadze & Menten 2012). V1478 Cyg is one of the brightest radio sources, and its emission at 2 cm shows an hourglass-shaped bipolar nebula (White & Becker 1985).

Besides a high-density ionized wind, V1478 Cyg displays strong IR excess emission, and near-IR speckle interferometry resolved a disc-like dust structure oriented in east–west direction, seen nearly edge-on (Leinert 1986; Mariotti et al. 1983). V1478 Cyg is unique in the sense that it is the only object with hydrogen recombination maser line emission in the mm and sub-mm range (e.g. Martín-Pintado et al. 1989). These masers originate from a dense gas disc, and the kinematics, obtained from their line profiles, imply Keplerian rotation of the disc (Thum, Martín-Pintado & Bachiller 1992,

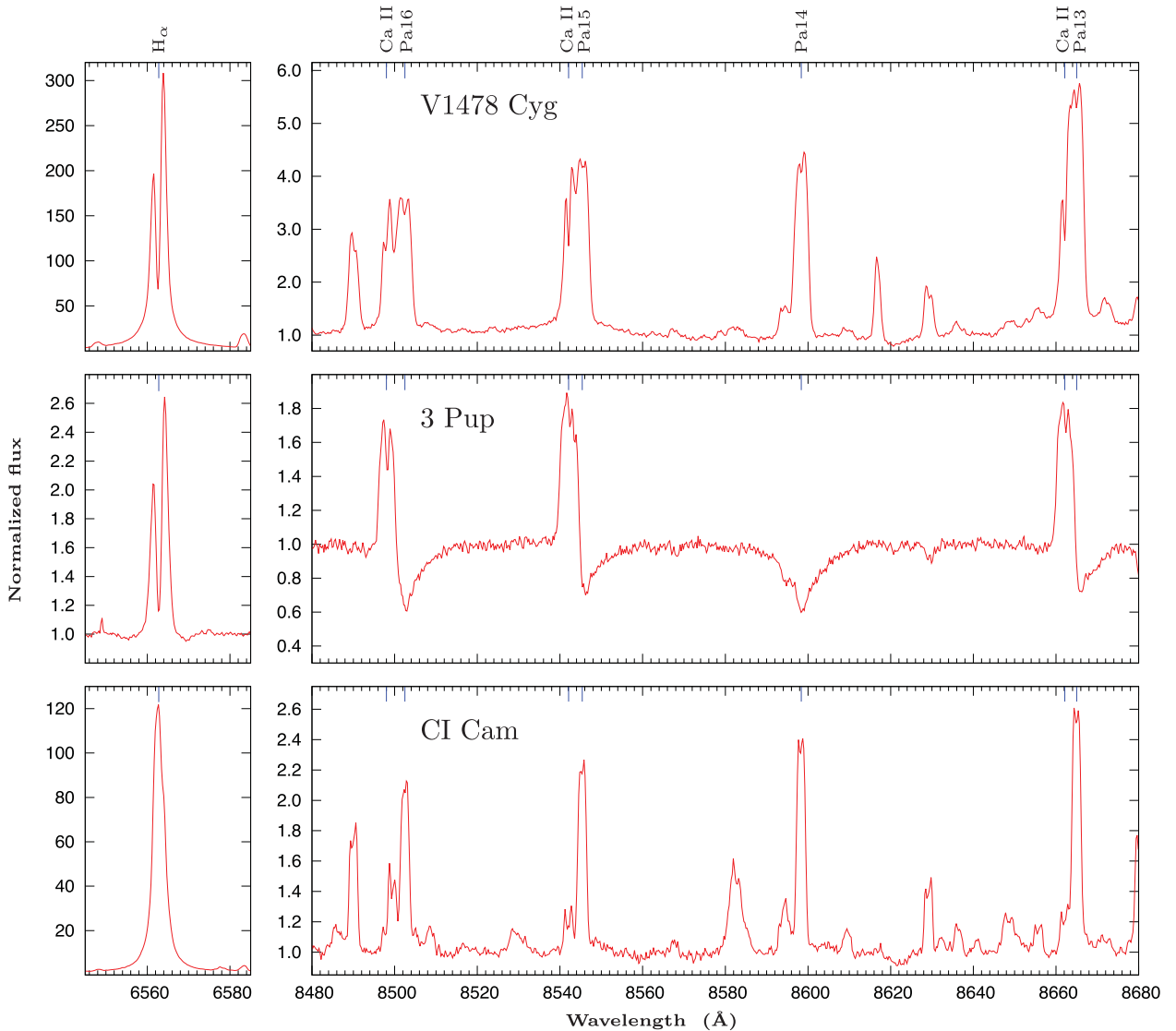


**Figure 4.** Spectral portions of B[e]SG stars covering the strategic lines of  $H\alpha$  and the  $\text{Ca II } \lambda\lambda 8498, 8542, 8662$  IR triplet. The wavelengths of the lines (including the four Pa lines) are marked by ticks. Spectra are corrected for heliocentric and systemic velocities.

Thum et al. 1994a), as well as a rotating wind emanating from the disc (Martín-Pintado et al. 2011; Báez-Rubio et al. 2013). Furthermore, CO-band emission has been detected (Geballe & Persson 1987; Kraus et al. 2000). The latter authors suggested that this emission originates from the far side of the inner molecular edge of the Keplerian disc.

Marston & McCollum (2008) discovered a thin  $H\alpha$  shell of approximately 2.5 arcmin diameter north of V1478 Cyg and a parsec-scale hourglass-shaped nebula is also seen in the mid-IR (Gvaramadze & Menten 2012; Strelitski et al. 2013). The observed characteristics favour an evolved nature of the star (Hofmann et al. 2002; Gvaramadze & Menten 2012). However, a pre-main-sequence evolutionary stage cannot be ruled out, based on the recently discovered proximity of V1478 Cyg to a molecular cloud with identical radial velocity (Strelitski et al. 2013).

V1478 Cyg displays a pure emission line spectrum in the wavelength ranges covered by our observations. With a line intensity of about 300 times the continuum, V1478 Cyg is the strongest  $H\alpha$  emitting source of our sample. The line profile is double peaked with the red peak about twice the intensity of the blue peak. The

Pa lines are narrow and slightly double peaked. They are blended with the  $\text{Ca II}$  IR triplet lines, which are also double peaked alike the  $[\text{Ca II}]$  lines. Only the  $[\text{O I}]$  lines show single-peaked profiles, but have been reported by Zickgraf (2003) to be slightly split as well when observed with (much) higher resolution. The diversity in the line profiles of the forbidden lines would be in agreement with the B[e]SG disc scenario of Aret et al. (2012) in which the  $[\text{O I}]$  lines formed farther away from the star (at smaller rotational velocity) than the  $[\text{Ca II}]$  lines.

### 3 Pup = MWC 570 = HD 62623

3 Pup is so far the only known Galactic A[e] supergiant. Emission from the  $\text{Ca II}$  IR triplet and the  $[\text{Ca II}]$  lines was seen by Hiltner (1947) and Danks & Dennefeld (1994), although the latter authors mistakenly identified the  $[\text{Ca II}]$  lines as the  $[\text{O II}]$  doublet lines. Based on radial velocity variations, Plets, Waelkens & Trams (1995) proposed that 3 Pup could be an interacting binary surrounded by gas and a dusty disc. Their analysis revealed an orbital period of either 131 or 161 d.

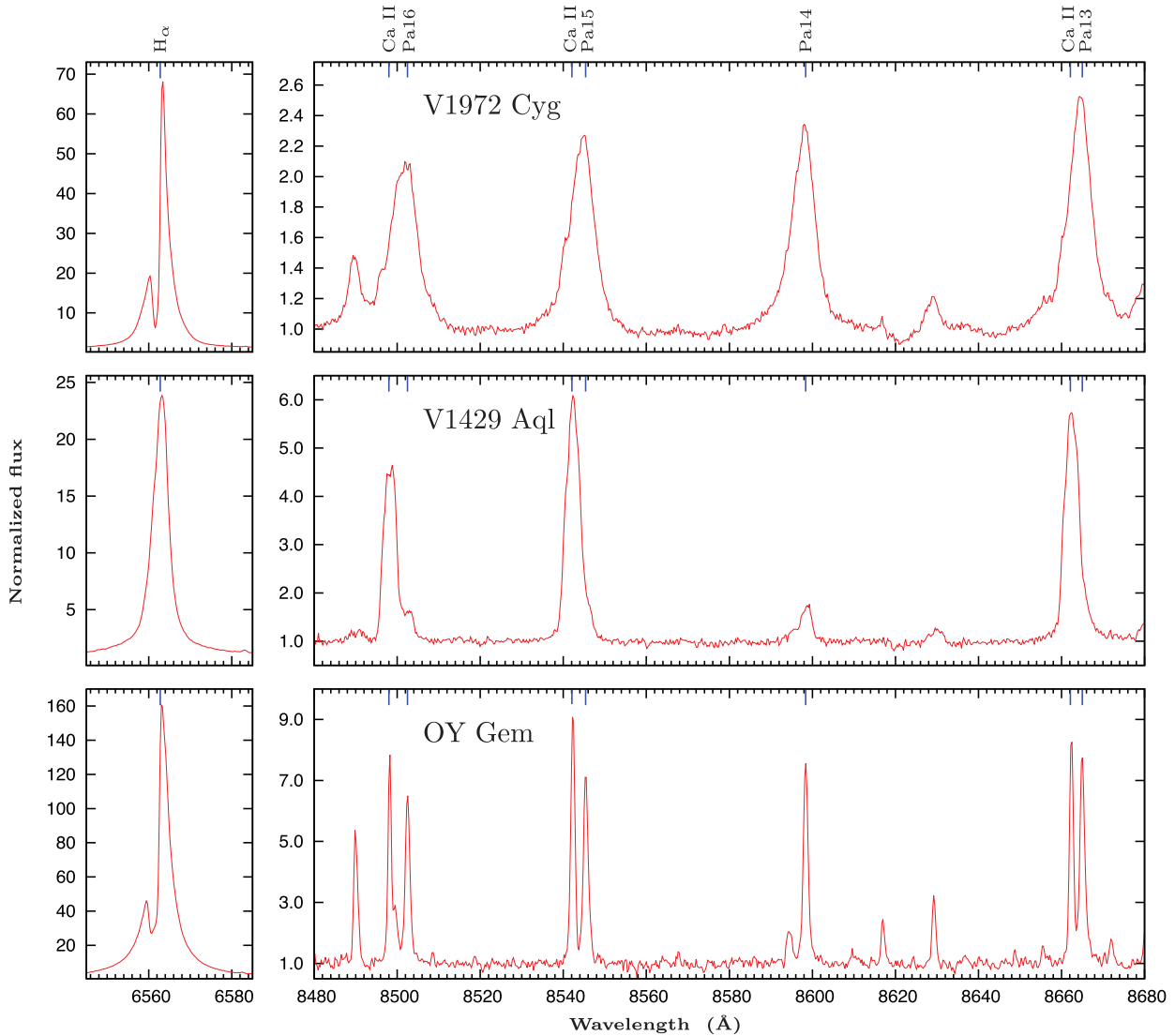


Figure 5. As Fig. 4, but for the two B[e]SG candidates and the compact planetary nebula.

No remarkable deviation from spherical symmetry of the dusty envelope was noticed by Monnier et al. (2004) implying that the disc is probably seen close to pole-on. Interferometric observations with VLTI/MIDI (Meilland et al. 2010) and VLTI/AMBER (Millour et al. 2011) resolved the disc and constrained the inclination angle to  $38^\circ$ . The disc consists of an inner, ionized gaseous part and an outer dusty part. This disc seems to be detached from the central star, as no emission was detected from the innermost region (Millour et al. 2011). This gap between star and disc could be caused by a close companion, as suggested from radial velocity variability (Plets et al. 1995). However, interferometry revealed no indication for such a companion (Millour et al. 2011). A double-peaked emission profile of Br  $\gamma$  was resolved by AMBER and clearly attributed to rotation of the gas disc (Millour et al. 2011). Double-peaked profiles were also reported for the optical emission lines from both permitted and forbidden transitions (Chentsov, Klochkova & Miroshnichenko 2010), as well as from CO band and SiO band emission in the near-IR region (Muratore et al. 2012b; Kraus et al. 2015), supporting the Keplerian rotating disc scenario.

Our spectra show that all strategic lines ([O I], [Ca II], Ca II IR triplet, and H  $\alpha$ ) are in emission with double-peaked profiles.

Remarkably, H  $\alpha$  has the least intensity of all our sample stars, supporting the results from the IR spectra, i.e. a lack of gas in the vicinity of the star. Its narrow emission profile is superimposed on a wider absorption profile. The peak separation of  $\sim 120 \text{ km s}^{-1}$  measured from our H  $\alpha$  profile agrees with the velocity obtained for Br  $\gamma$  (Millour et al. 2011). Hence, both lines should originate from the same region, i.e. from the detached gas ring resolved by interferometry (Millour et al. 2011). The Pa lines are in pure absorption. Their broad wings are blended with the emission from the Ca II IR triplet lines. The appearance of both sets of forbidden emission lines indicates a high density within the gaseous disc of 3 Pup.

#### CI Cam = MWC 84

The star CI Cam was identified as the optical counterpart of the X-ray source XTE J0421+560. It is an eccentric binary system consisting of a bright optical object and a compact companion, possibly a white dwarf (e.g. Ishida, Morio & Ueda 2004). Barsukova et al. (2006) derived a period of 19.41 d and an eccentricity of 0.62. Furthermore, they suggested the primary to be a massive ( $> 12 M_\odot$ ) star.

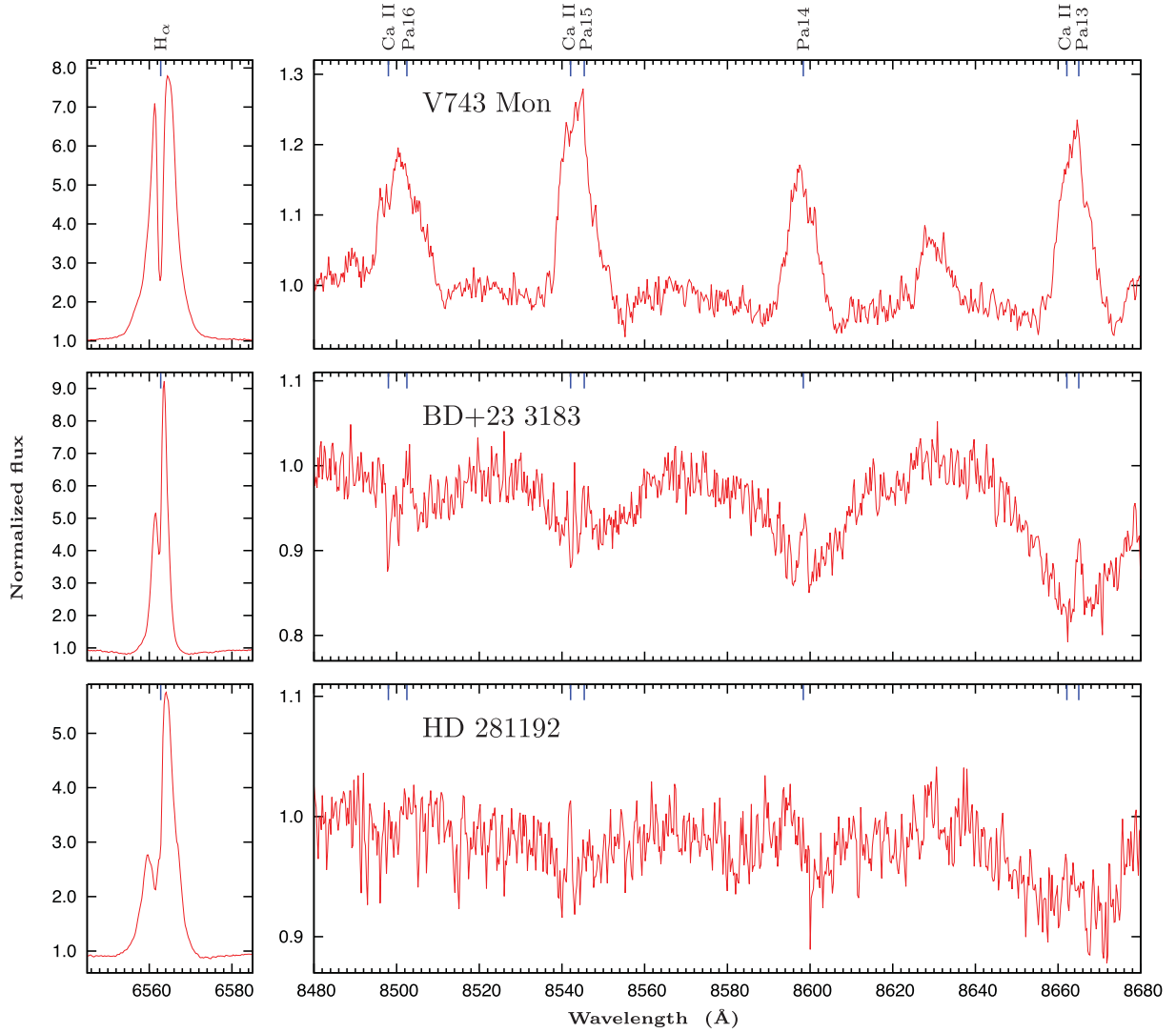


Figure 6. As Fig. 4, but for the unclassified B[e] stars.

**Table 3.** Shapes (Sh), peak separations (PS, in  $\text{km s}^{-1}$ ), full widths at zero intensity (ZI, in  $\text{km s}^{-1}$ ) and full widths at half-maximum (HM, in  $\text{km s}^{-1}$ ) of forbidden oxygen and calcium lines. Errors are shown as superscript. Classification of the line profile types: S – single-peaked emission line; D – double-peaked emission line; W – weak emission line with unclear (not resolved) profile shape; X – no line detected.

Object	[O I] 6300 Å				[O I] 6364 Å				[Ca II] 7291 Å				[Ca II] 7324 Å			
	Sh	PS	ZI	HM	Sh	PS	ZI	HM	Sh	PS	ZI	HM	Sh	PS	ZI	HM
V1478 Cyg	S	–	150 <sup>10</sup>	63 <sup>2</sup>	S	–	160 <sup>15</sup>	68 <sup>2</sup>	D	n.r.	150 <sup>20</sup>	80 <sup>5</sup>	D	41 <sup>1</sup>	140 <sup>20</sup>	90 <sup>5</sup>
3 Pup	D	48 <sup>5</sup>	165 <sup>10</sup>	105 <sup>5</sup>	W	–	190 <sup>25</sup>	93 <sup>10</sup>	D	65 <sup>8</sup>	147 <sup>15</sup>	105 <sup>8</sup>	D	56 <sup>5</sup>	150 <sup>15</sup>	95 <sup>8</sup>
CI Cam	X	–	–	–	X	–	–	–	X	–	–	–	X	–	–	–
V1972 Cyg	S	–	143 <sup>5</sup>	45.6 <sup>1</sup>	S	–	144 <sup>5</sup>	45.5 <sup>1</sup>	X	–	–	–	X	–	–	–
V1429 Aql <sup>a</sup>	W	–	140 <sup>20</sup>	61 <sup>5</sup>	X	–	–	–	D	61 <sup>2</sup>	156 <sup>5</sup>	105 <sup>3</sup>	D	62 <sup>2</sup>	146 <sup>5</sup>	109 <sup>2</sup>
OY Gem	S	–	120 <sup>10</sup>	39 <sup>2</sup>	S	–	115 <sup>10</sup>	37 <sup>2</sup>	S	–	80 <sup>10</sup>	27 <sup>1</sup>	S	–	70 <sup>5</sup>	24 <sup>1</sup>
V743 Mon	S	–	156 <sup>6</sup>	52 <sup>1</sup>	S	–	142 <sup>13</sup>	51 <sup>1</sup>	X	–	–	–	X	–	–	–
BD+23 3183	S	–	150 <sup>10</sup>	120 <sup>10</sup>	S	–	120 <sup>10</sup>	41 <sup>5</sup>	X	–	–	–	X	–	–	–
HD 281192 <sup>b</sup>	S	–	160 <sup>10</sup>	78 <sup>1</sup>	S	–	170 <sup>20</sup>	80 <sup>2</sup>	X	–	–	–	X	–	–	–

Notes. <sup>a</sup>Identification of the [O I] 6300 Å line uncertain.

<sup>b</sup>Indication of a slightly (but unresolved) double-peaked profile of the [O I] lines.

CI Cam became famous due to its spectacular outburst in 1998 over the complete wavelength range, from  $\gamma$ -ray to radio, during which the object brightened by 2–3 magnitudes. At that time, optical (e.g. Robinson, Ivans & Welsh 2002) and IR spectroscopy

(e.g. Clark et al. 1999) revealed a rich emission line spectrum that changed drastically with time, indicating a highly dynamical environment, dense enough to hide the central star. Most of the emission lines presented triple-peaked profiles, suggesting a gas disc seen



**Table 4.** Shapes of H  $\alpha$  and Ca II IR triplet lines. Classification of the line profile types: S – single-peaked emission line; D – double-peaked emission line; B – emission line strongly blended with Pa line, no classification possible; DWA – double-peaked emission line on top of wide absorption component; X – no line detected.

Object	H $\alpha$	Ca II 8498 Å	Ca II 8542 Å	Ca II 8662 Å
V1478 Cyg	D	D	D	D
3 Pup	DWA	D	D	D
CI Cam	S	D	D	D
V1972 Cyg	D	B <sup>a</sup>	B <sup>a</sup>	B <sup>a</sup>
V1429 Aql	S	S	S	S
OY Gem	D	S	S	S
V743 Mon	D	B	B	B
BD+23 3183	DWA	X	X	X
HD 281192	DWA	X	X	X

Note. <sup>a</sup>Identification uncertain.

under an intermediate inclination angle, and an additional dense, probably ring-shaped region farther away from the star (Miroshnichenko et al. 2002). Strong near- and mid-IR excess emission due to circumstellar dust was reported by Allen (1973). Hynes et al. (2002) concluded that this dust must be located in the outer region of the gas disc, and follow-up studies using long baseline optical interferometry in the *H* and *K* spectral bands confirmed that the hot dust is confined within a skewed, asymmetric ring (Thureau et al. 2009).

Based on the spectral properties and the existence of a molecular and dusty disc, the primary of CI Cam was suggested by Clark et al. (1999) and Hynes et al. (2002) to belong to the group of B[e]SGs. Indication for the typical two-component B[e]SG wind (see Zickgraf et al. 1985) was found by Robinson et al. (2002) and Hynes et al. (2002). Marston & McCollum (2008) discovered an extended faint H  $\alpha$  shell around CI Cam. However, proper spectral classification of the B[e]SG component turned out to be difficult due to the uncertain distance and the absence of photospheric lines. Barsukova et al. (2006) derived a spectral type of B4 III–V, but the spectral energy distribution is also in agreement with an earlier classification of B0–B1 III by Thureau et al. (2009), while Hynes et al. (2002) obtained B0–B2 I and a luminosity of  $\log L/L_{\odot} \gtrsim 5.4$ .

**Table 5.** Stellar parameters of the sample stars.

Star	$T_{\text{eff}}$ (K)	$\log L/L_{\odot}$	$M_*$ ( $M_{\odot}$ )	Disc	$i^a$ ( $^{\circ}$ )	CO bands	Reference
V1478 Cyg	$24\,000 \pm 4000$	$5.75 \pm 0.15$	38	Yes	82	Emis	(1), (2), (3), (4)
3 Pup	$8250 \pm 250$	$4.33 \pm 0.09$	15–20	Yes	38	Emis	(5), (6)
CI Cam	$24\,000 \pm 6000$ $20\,000 \pm 2000$	$> 5.4$ $< 4.0$	$> 12$	Possibly <sup>b</sup> Uncertain	$\sim 0$	Emis No	(7), (8) (9), (10)
V1972 Cyg	26 000	$4.2 \pm 0.4$	–	Uncertain	–	No	(11), (12), (13)
V1429 Aql	18 000	5.85	$66 \pm 9^c$	Yes	$73 \pm 13$	No	(14), (15), (10)
OY Gem	28 000	3.8	0.62	Uncertain	–	No	(16), (17)
V743 Mon	$13\,200 \pm 500$	$3.06 \pm 0.27$	5	Yes	$56 \pm 4$	No	(18), (19), (6)
BD+23 3183	10 000	$< 4$	$< 4$	Uncertain	–	Unknown	(20)
HD 281192	14 000	–	$4 \pm 0.5$	Uncertain	–	Abs	(21), (22)

Notes. <sup>a</sup>Inclination angle of the system rotation axis with respect to the line of sight. Inclination of  $90^{\circ}$  means edge-on view of the disc.

<sup>b</sup>During the outburst phase. <sup>c</sup>Total mass of the binary system.

References: (1) Hofmann et al. (2002); (2) Báez-Rubio et al. (2013); (3) Geballe & Persson (1987); (4) Kraus et al. (2000); (5) Millour et al. (2011); (6) Muratore, Kraus & de Wit (2012a); (7) Hynes et al. (2002); (8) Clark et al. (1999); (9) Miroshnichenko et al. (2002); (10) Liermann et al. (2014); (11) Miroshnichenko & Corporon (1999); (12) Oudmaijer et al. (2005); (13) Arias, private communication; (14) Lobel et al. (2013); (15) Muratorio et al. (2008); (16) Arhipova & Ikonnikova (1992); (17) Venkata Raman & Anandarao (2008); (18) Borges Fernandes et al. (2009); (19) Borges Fernandes et al. (2011); (20) Miroshnichenko et al. (2007); (21) Miroshnichenko et al. (2015); (22) Arias et al. in preparation.

Our spectra for CI Cam display numerous, narrow emission features, most of them single peaked. The Pa lines and the adjacent lines from the Ca II IR triplet appear slightly double peaked. None of the lines in the spectral regions covered by our observations show the triple-peaked profiles reported by Miroshnichenko et al. (2002), but it can also be caused by the lower resolution of our spectra. The similarity of our data to those obtained in 1987 (the pre-outburst phase) by Zickgraf (2003), who observed the same profile of the H  $\alpha$  line and reported on the lack of noticeable [O I] emission, indicates that the system is back in its pre-outburst phase. This could mean that during the last few years, the conditions in the circumstellar matter have changed, i.e. parts of the ejected gaseous material probably expanded and diluted. Evidence for such a scenario comes also from recent observations in the near-IR spectral range, which revealed that CI Cam lost its CO band emission (Liermann et al. 2014). Expansion and dilution of the previously ejected material would also explain why we could not detect any emission in either [Ca II] or [O I].

### V1972 Cyg = MWC 342

This star was identified by Merrill & Burwell (1933) as an emission-line object, being either in the pre-main sequence (Herbig Ae/Be star; Bergner et al. 1990) or in an evolved evolutionary phase, perhaps as part of a binary system (Miroshnichenko & Corporon 1999).

Optical and IR polarization is very small, hinting towards some slight asymmetries of the envelope (Bergner et al. 1990; Oudmaijer, Drew & Vink 2005), but providing no clear indication for presence of an ionized circumstellar disc. Marston & McCollum (2008) found a faint H  $\alpha$  shell around that star. *K*-band observations display strong emission of the hydrogen Pfund series, but no CO-band emission (Arias, private communication). These characteristics are similar to the LBV candidate V1429 Aql (Liermann et al. 2014) and other LBV stars surveyed in the near-IR so far (Oksala et al. 2013).

Our spectra of V1972 Cyg display strong emission of H  $\alpha$  and the Pa lines. H  $\alpha$  is double peaked with the red peak about 3.5 times more intense than the blue one. The Pa lines display prominent broad, but single-peaked profiles with extended wings, which are strongly blended with the lines of the Ca II IR triplet. No [Ca II] lines were detected. The [O I] lines appear as intense, narrow, single-peaked emission features. Their possible split of  $10 \text{ km s}^{-1}$  reported by

Zickgraf (2003) from high-resolution data, cannot be resolved. Such a split of the forbidden emission lines implies that they are formed either in a rotating ring or an equatorial outflow of dense, neutral gas. The absence of the [Ca II] lines indicates that the circumstellar gas must be less dense than in typical B[e]SGs, and the lack of molecular emission implies that the circumstellar material is not confined within a disc or ring.

### V1429 Aql = MWC 314

The object V1429 Aql was discovered by Merrill (1927) as a star showing bright iron lines. The stellar parameter determination via the Balmer discontinuum method failed due to the crowded emission line spectrum (Cidale, Zorec & Tringaniello 2001). Alternative methods revealed a temperature ranging from 32 000 K, based on the He I lines, to 26 700 K, when considering the visible line spectrum and energy distribution. The latter is close to the value of 25 000 K suggested by Miroshnichenko et al. (1998), while Carmona et al. (2010) found a much lower value of 16 200 K.

Earlier optical spectroscopic observations reported symmetric Balmer lines, He I lines, and numerous, mainly double-peaked lines from permitted and forbidden transitions in neutral and low-ionized metals, including the lines of the Ca II IR triplet (Miroshnichenko et al. 1998; Carmona et al. 2010). The presence of the [Ca II] lines was suggested by Miroshnichenko et al. (1998), but their spectra suffer from telluric pollution, altering the shapes and strengths of these lines.

The double-peaked line profiles imply a non-spherical symmetry of the wind, and H  $\alpha$  imaging by Marston & McCollum (2008) revealed a very large bipolar nebula structure with approximately 15 arcmin in total length. Considering a distance of  $\sim 3$  kpc, this results in a total extension of the bipolar structure of 13.5 pc from end to end, which is about five times larger than sizes of typical LBV nebulae. Bipolarity is also often observed in LBVs, and the morphology of the bipolar nebula around V1429 Aql strongly resembles the one seen around  $\eta$  Car, suggesting that a circumstellar disc could have caused the shaping of the nebula. A rotating disc hypothesis is also supported by the line formation studies by Muratorio, Rossi & Friedjung (2008). However, if present at all, dust does not provide a major constituent of this disc because the spectral energy distribution shows no indication for an IR excess due to circumstellar dust. The absence of measurable amount of dust implies that V1429 Aql is not a classical B[e]SG candidate.

Indeed, Lobel et al. (2013) found that V1429 Aql is a massive semidetached binary ( $P = 60.8$  d, eccentricity  $e = 0.23$ , total mass  $M \simeq 66 \pm 9 M_{\odot}$ , and maximum distance between stars  $a = 1.22$  au), consisting of a hot (18 000 K) and luminous ( $7.1 \times 10^5 L_{\odot}$ ) primary star (possibly in an LBV-like state) with mass  $\sim 40 M_{\odot}$ , and a cool ( $\sim 6300$  K) secondary with mass  $\sim 26 M_{\odot}$ . With an inclination angle of  $17^{\circ} \pm 13^{\circ}$ , the system is seen almost equator on, as is also inferred from the light-curve characteristic for an eclipsing system. The inclination angle also agrees with the value of  $25^{\circ} \pm 5^{\circ}$  suggested by Muratorio et al. (2008) for the orientation of the rotating (circumbinary) gas disc. The period of the system was confirmed by Frasca et al. (2015) who obtained  $P = 60.7$  d based on detailed analysis of absorption and emission lines in spectra covering a period of about 15 years.

Investigations of the near-IR appearance of V1429 Aql revealed that it shows strong emission in the hydrogen Pfund series, while no indication for CO-band emission could be found (Liermann et al. 2014). Such a behaviour seems to be typical for LBVs (Oksala et al. 2013), supporting the LBV classification of V1429 Aql.

Both the LBV status of the primary as well as the masses of the binary components were recently questioned by Richardson et al. (2016), based on combined spectroscopic, interferometric, and photometric observations. While the results of Lobel et al. (2013) are a possible solution, Richardson et al. (2016) propose a much lower total mass of the system of  $20 M_{\odot}$  only and a mass ratio  $M_2/M_1 = 3$ , and suggest that strong mass transfer in an interacting binary could have caused the reversal. However, the authors state that their investigations provide no unique solution and more observations are definitely needed to resolve this issue.

Our data show no clear evidence for [O I] line emission in agreement with the earlier observations. This is another indicator that V1429 Aql is not a typical B[e]SG. H  $\alpha$  and the Pa lines are in emission and have a symmetric single-peaked profile shape. The strength of the H  $\alpha$  line is comparable to the one of Miroshnichenko et al. (1998), but stronger than the one reported by Carmona et al. (2010). Variability in H  $\alpha$  and R-band polarization on time-scales of days to weeks has been notified by Wisniewski et al. (2006). The origin of this variability could be due to the binarity (Wisniewski et al. 2006; Muratorio et al. 2008; Lobel et al. 2012), while other studies suggest V1429 Aql might perform non-periodic pulsations as they appear in strange modes, typical for LBVs (Rossi et al. 2011). Furthermore, our spectra display strong emission in both the Ca II IR triplet lines and the [Ca II] lines. While the profiles of the triplet lines appear symmetric and single peaked, those of the forbidden lines are clearly double peaked with the blue peak slightly more intense due to blending with adjacent emission lines.

### OY Gem = MWC 162 = HD 51585

The object OY Gem was discovered as an emission-line star by Merrill & Burwell (1933). Many forbidden emission lines (including lines of [O I] and [Ca II]) from transitions covering a large range in excitation energies have been identified in extensive spectroscopic observations (see e.g. Klutz & Swings 1977; Arkhipova & Ikonnikova 1992; Jaschek, Andrillat & Jaschek 1996). The object displays IR excess emission (Allen & Swings 1976), but no indication for extended H  $\alpha$  emission (Marston & McCollum 2008).

Photometry and emission line strengths display strong variability on different time-scales (see e.g. Arkhipova et al. 2006), which are interpreted as due to variability in the stellar wind. Wheelwright, Oudmajer & Goodwin (2010) found indication for a companion based on spectroastrometric observations. They list OY Gem as a Herbig Ae/Be star. However, Herbig Ae/Be and post-AGB (asymptotic giant branch) stars have many common emission features in their spectra. And in fact, high-ionization forbidden emission lines, the presence of two detached shells (Arkhipova & Ikonnikova 1992; Venkata Raman & Anandarao 2008) with hot (1100–1200 K) and cold (150–180 K) carbon-rich dust detected with *Spitzer* (Cerrigone et al. 2009), and the absence of any spectroscopic evidence for accretion over the last decades clearly speak in favour of classification as post-AGB or compact planetary nebula rather than as a pre-main-sequence object.

The forbidden lines in our spectra of OY Gem are sharp and single peaked. The exception is H  $\alpha$ , which has a double-peaked profile with the red peak  $\sim 3.5$  times the intensity of the blue one. The intensity of the H  $\alpha$  line in OY Gem is among the strongest in our sample. Furthermore, the wings of the H  $\alpha$  line extend to large velocities ( $\sim 3200 \pm 100$  km s $^{-1}$ ). Such broad wings (of  $\sim 2900$  km s $^{-1}$ ) have also been reported by Swings & Andrillat (1981), not only for H  $\alpha$ , but also for higher Balmer lines. In contrast, the Pa lines are very narrow and only slightly blended with the

equally narrow Ca II IR triplet lines. OY Gem has by far the strongest [O I] and [Ca II] lines of all our sample stars, comparable to those typically seen in post-AGB stars.

#### V743 Mon = MWC 158 = HD 50138

The star V743 Mon belonged to the group of unclassified B[e] stars for a long time. It displays strong spectral as well as small-scale photometric variabilities, which are suggested to be caused by shell phases of the star (e.g. Andriillat & Houziaux 1991; Borges Fernandes et al. 2009), and at least one larger outburst was recorded in 1978/79 (Hutsemekers 1985). However, no extended H  $\alpha$  emission was detected by Marston & McCollum (2008).

V743 Mon has often been referred to as a Herbig (hence pre-main-sequence) star, but the lack of a close-by star-forming region in combination with regular shell phases of the star, which are not observed in pre-main-sequence stars, make such a classification rather doubtful. V743 Mon was recently re-classified by Borges Fernandes et al. (2009) as a B6–7 III–V star of  $\sim 5 M_{\odot}$ , located at the end of the main sequence. An extended, dusty disc, seen under an inclination of  $56^{\circ} \pm 4^{\circ}$ , was discovered by Borges Fernandes et al. (2011). Based on spectroastrometric observations, Baines et al. (2006) suggested that V743 Mon could be a binary system. However, no indication for a companion has been found from either spectroscopic or interferometric observations (Borges Fernandes et al. 2011). As an additional curiosity, the recent analysis of line-profile variability of photospheric lines suggests that the star could be pulsating (Borges Fernandes et al. 2012). The confirmation is, however, still pending.

The shape of the H  $\alpha$  line profile agrees with the presence of a gaseous disc seen at intermediate inclination. The Pa lines are broad and seem to consist of multiple components. Emission in the Ca II IR triplet lines seems to be present, but these lines are strongly blended with the Pa lines, while the [Ca II] lines are absent. The [O I] lines are narrow and single peaked.

#### BD+23 3183 = IRAS 17449+2320

Not much is known yet about the object BD+23 3183. It was discovered as a new H  $\alpha$  emission-line star by Stephenson (1986), who listed it as number 145 in his catalogue. Downes & Keyes (1988) performed a follow-up low-resolution optical spectroscopic study in which they classify it as Be star. The detection of a strong IR excess and of [O I] emission resulted in the classification as B[e] star (Miroshnichenko et al. 2007). Other lines such as Fe II, He I, and Mg II were in pure absorption, suggesting a spectral type of A0 and classification as a dwarf star.

Our spectra confirm the presence of [O I] and Balmer line emission. However, compared to the observations by Miroshnichenko et al. (2007) the blue peak of our H  $\alpha$  line is much less intense. The Pa lines display small and narrow central emission features superimposed on the broad photospheric absorption component similarly to what was seen for H  $\beta$  (Miroshnichenko et al. 2007). The H  $\alpha$  emission line shows also indication for an underlying photospheric absorption component, extending to higher velocities than the emission wings. The spectra show no evidence for calcium line emission, neither in [Ca II] nor in the Ca II IR triplet.

#### HD 281192 = MWC 728

The object HD 281192 was first detected as an emission-line star by Merrill & Burwell (1949) and listed in their second supplement

to the Mount Wilson Catalogue of early-type emission-line stars. Although HD 281192 shares its *IRAS* colours with typical OH/IR stars, no OH maser lines were detected by Chengalur et al. (1993). Miroshnichenko et al. (2007) obtained high-resolution optical spectra and reported the emission of double-peaked profiles of [O I] and the Balmer lines, while the iron lines were in pure absorption. Furthermore, from the presence of weak absorption features of Li I and Ca I these authors propose a binary nature of HD 281192. Support for a companion is also provided by recent *K*-band spectra, which revealed CO bands in absorption (Arias et al., in preparation), typically seen from the atmospheres of late-type giants. Indeed, Miroshnichenko et al. (2015) found that the system consists of a B5 Ve primary and a G8 III secondary, and has an orbital period of 27.5 d. They also report on non-periodic variability of the emission lines.

Our spectra confirm the presence of pronounced, narrow [O I] lines and a double-peaked H  $\alpha$  emission with the red peak about twice as intense as the blue peak. The emission is superimposed on a much wider absorption. Our [O I] lines are single-peaked, but our spectra have lower resolution than those obtained by Miroshnichenko et al. (2007, 2015). The shape of the emission features in our spectra are very similar to those in BD+23 3183, but the intensities of H  $\alpha$  and the [O I] lines in BD+23 3183 are approximately twice and half as strong, respectively. No indication for [Ca II] or the Ca II IR triplet is found.

## 4 DISCUSSION

The former studies of forbidden emission lines in a sample of B[e]SGs by Aret et al. (2012) revealed that the kinematics, derived from the line profiles, agrees with the scenario of a Keplerian rotating disc, in which the [Ca II] lines are formed closest to the star, followed by the [O I]  $\lambda 5577$  line and the [O I]  $\lambda \lambda 6300, 6364$  lines. The hypothesis of Keplerian rotation of these circumstellar discs is further supported by near-IR studies, focused on the molecular CO band emission, which shows indication for rotational broadening as well (Cidale et al. 2012; Muratore et al. 2012b, 2015; Wheelwright et al. 2012; Kraus et al. 2013; Oksala et al. 2013).

Only three objects in our sample display emission in the two strategic sets of forbidden lines, [O I] and [Ca II]. These are the two B[e]SGs V1478 Cyg and 3 Pup, and the compact planetary nebula star OY Gem. The LBV candidate V1429 Aql only displays the [Ca II] lines, but no [O I] emission. Except for OY Gem, all these stars are confirmed disc sources (see Table 5), and the line profiles clearly show kinematic broadening. The remaining object with confirmed disc in our sample, V743 Mon, has only the B[e] star characteristic [O I] emission. As the line profile is single peaked, no reliable constraints with respect to the kinematics in the line-forming region can be obtained.

In the remaining, we focus on the objects with [Ca II] emission. For clearer inspection of the line profile shapes, we subtracted the continuum and scaled the line intensities to unity. These profiles are displayed in Fig. 7. In both B[e]SGs, the [Ca II] line is clearly double peaked and broader than the [O I] line, in agreement with the Keplerian disc scenario for this type of objects. Also in V1429 Aql, the [Ca II] lines have double-peaked profiles. Because our spectra have only medium resolution ( $\sim 23 \text{ km s}^{-1}$  at [O I] and  $\sim 20 \text{ km s}^{-1}$  at [Ca II]), the peak separation, listed in Table 3, does not provide proper rotational velocities. Therefore, we applied a simple, purely kinematic model to compute line profiles for comparison with the observations. Assuming that the emission originates from a narrow (i.e. constant velocity) rotating ring, we calculate the profile shape considering only rotational velocity, projected to the line of sight

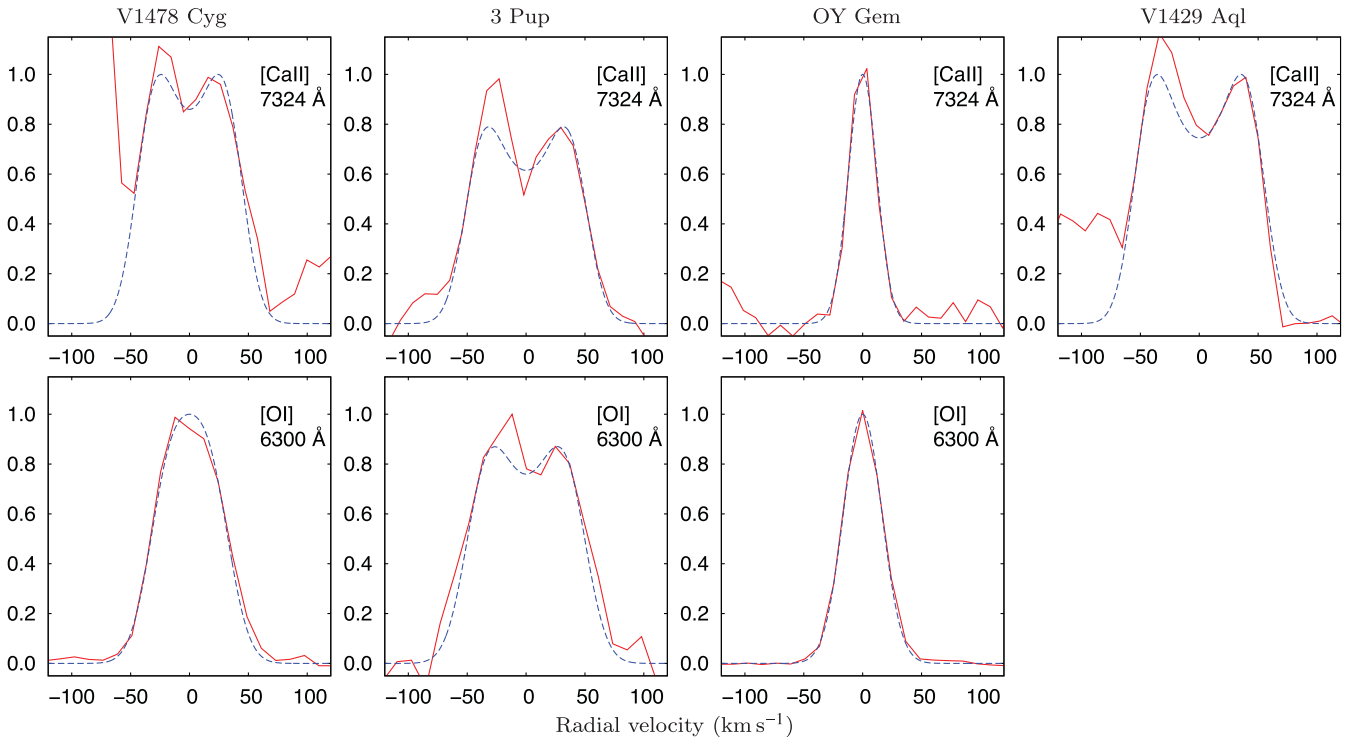


**Figure 7.** Kinematic model fits (dashed blue) to the observed profiles (solid red) of the forbidden lines.

according to the observed inclination angles (Table 5), and the resolution of the spectrograph. In all cases, we obtain good fits to the observed line profiles, demonstrating that the observed emission originates indeed from a narrow ring region. These fits are included in Fig. 7, and the corresponding rotational velocities are listed in Table 6. Also listed are the corresponding radii of the emitting rings assuming Keplerian rotation.

For OY Gem, no kinematic broadening beyond the spectral resolution was needed to fit the line profile shapes. If this object has a disc, it must be oriented pole-on. Or, if the emission originates from a shell, that was ejected during the former AGB phase, the expansion velocity of the material must have decelerated to (almost) zero. High-resolution spectra are clearly needed to properly resolve profile shapes and to investigate the kinematics.

Despite the reported disc around the LBV candidate V1429 Aql (MWC 314) and the detection of the [Ca II] lines, no [O I] lines are observed. This could indicate that the gas disc around this massive, luminous object is too hot for hydrogen (hence oxygen) to exist in its neutral state at an amount sufficient for detection. Considering the mass estimates and binary separation by Lobel et al. (2013), the

emission region of [Ca II] must clearly be circumbinary, and from our rotational velocity we obtain a distance of  $23.4 \pm 4$  au.

The B[e]SG V1478 Cyg (MWC 349A) is surrounded by a large (0.05–130 au) Keplerian rotating disc, consisting of an ionized surface layer and a cool, neutral, and dusty mid-layer, at least in the outer regions. Moreover, a wind is ejected from the ionized disc at a radius of  $\sim 24$  au, with a terminal outflow velocity of  $60 \text{ km s}^{-1}$ , and rotating in the same sense as the disc (Báez-Rubio et al. 2013, 2014). With the recent, new mass estimates of  $38\text{--}40 M_{\odot}$  (Gvarnadamze & Menten 2012; Báez-Rubio et al. 2013), we locate the [Ca II] emission region at a distance of  $24.6 \pm 1.3$  au, which coincides with (or is just beyond) the region, from which the wind is launched. The Keplerian velocity obtained for [O I] agrees with the values obtained for several hydrogen recombination maser lines (e.g. Thum et al. 1994a,b, 1995). The distance of their emission regions amounts to  $55.7 \pm 5.9$  au.

The rotational velocities of the forbidden lines in 3 Pup, when combined with those obtained from CO-band ( $53 \text{ km s}^{-1}$ ; Muratore et al. 2012b) and SiO-band emission ( $48 \text{ km s}^{-1}$ ; Kraus et al. 2015), provide the best example for tracing the Keplerian gas disc from the atomic to the molecular region. However, proper distance determination of the emission regions is hampered by the uncertain mass (luminosity) of the central object. Millour et al. (2011) determined a value of  $15\text{--}20 M_{\odot}$  and a distance of 650 pc. The kinematically resolved gas disc would thus extend from  $3.0 \pm 0.4$  au ([Ca II]) to  $6.7 \pm 1.0$  au (SiO). This parameter combination would place (parts of) the atomic and molecular emission regions beyond the inner edge of the dusty disc, which is suggested to be at about 4 au (Millour et al. 2011). However, the temperatures of these molecular regions clearly exceed the dust sublimation temperature, and should hence be located closer to the star than the dusty part.

This inconsistency can only be resolved for either a lower mass of the central object or a greater distance (or a combination of both). Chentsov et al. (2010) have determined a slightly greater

**Table 6.** Disc kinematics.

Star	[Ca II] $v_{\text{rot}}(\text{km s}^{-1})$	[O I] R (au)	$v_{\text{rot}}(\text{km s}^{-1})$	R (au)
V1478 Cyg	$38 \pm 1$	$24.6 \pm 1.3$	$25 \pm 1$	$55.7 \pm 5.9$
3 Pup	$72 \pm 1$	$3.0 \pm 0.4^a$ $1.67 \pm 0.13^b$	$68 \pm 1$	$3.4 \pm 0.5^a$ $1.87 \pm 0.14^b$
V1429 Aql	$50 \pm 1$	$23.4 \pm 4.0$	–	–
OY Gem	0	–	0	–

Notes. <sup>a</sup>Using the mass range of Millour et al. (2011);

<sup>b</sup>using a mass range of  $9\text{--}10.5 M_{\odot}$ , see Section 4.

distance of 700 pc, a spectral type of  $A2.7 \pm 0.3$  Ib, and a value of  $M_V = -5.5 \pm 0.3$ . This results in a luminosity value of  $\log L/L_\odot = 4.10 \pm 0.12$ . Assigning the total luminosity to the massive component, a mass can be estimated from a comparison with stellar evolutionary tracks from Ekström et al. (2012) for single rotating stars with solar metallicity. This delivers a possible mass range of 9–10.5  $M_\odot$ . The kinematically traced disc would thus extend from  $1.67 \pm 0.13$  au ([Ca II]) to  $3.75 \pm 0.29$  au (SiO), while the slightly greater distance to the object would place the inner edge of the dusty disc at 4.2 au, hence providing a more consistent scenario.

## 5 CONCLUSIONS

In our survey of B[e] stars, we detect emission of the strategic [Ca II] lines in four out of a sample of nine objects. Three of these objects with [Ca II] emission are known to possess circumstellar discs, and the kinematics derived from the line profiles agree with Keplerian rotation. Two of these sources, V1478 Cyg and 3 Pup, are B[e]SGs, while the third one, V1429 Aql, is an LBV candidate. The fourth object, OY Gem, is a known compact planetary nebula. If it has a disc, it should be oriented pole-on, because no kinematic broadening was detected beyond spectral resolution.

Another object of this survey is CI Cam, which was reported by Clark et al. (1999) and Hynes et al. (2002) to show all characteristics typically seen in B[e]SGs after it had experienced an outburst. This star shows no indication for either [Ca II] or [O I] emission in our spectra, in line with the reported disappearance of its CO-band emission. This suggests that CI Cam is back in its pre-outburst state.

Our sample also contains three B[e] stars with unclear evolutionary stage. None of them has the [Ca II] lines, and only the disc source V743 Mon displays emission in the Ca II IR triplet. Based on the results of Aret et al. (2012) and also those presented here, the [Ca II] lines tend to appear in regions closer to the star than the [O I] lines, i.e. in regions of higher density. The lack of measurable amounts of emission from these non-massive stars might hence indicate that their circumstellar environments have not the proper physical conditions in terms of density and size of the emitting volume.

The detection of the strategic forbidden lines, particularly in massive stars which have circumstellar environments with high density and rather large volume, as it is the case in the discs of B[e]SGs, strengthens their importance as valuable disc tracers. Hence, these lines provide an ideal tool to identify objects with similar circumstellar environments, and allow us to study the physical conditions and kinematics within their line forming regions.

## ACKNOWLEDGEMENTS

We thank the technical staff at the Ondřejov Observatory for the support during the observations. We thank the referee for useful comments that helped to improve the presentation of our results. This research made use of the NASA Astrophysics Data System (ADS) and of the SIMBAD data base operated at CDS, Strasbourg, France. MK acknowledges financial support from GA ČR under grant number 14-21373S and from the European Structural Funds grant for the Centre of Excellence ‘Dark Matter in (Astro)particle Physics and Cosmology’. The Astronomical Institute Ondřejov is supported by the project RVO:67985815. AA acknowledges financial support from Estonian Science Foundation grant ETF8906. This work was also supported by the research projects SF0060030s08 and IUT40-1 of the Estonian Ministry of Education and Research.

## REFERENCES

- Allen D. A., 1973, *MNRAS*, 161, 145  
 Allen D. A., Swings J. P., 1976, *A&A*, 47, 293  
 Andriillat Y., Houziaux L., 1991, *IAU Circ.*, 5164, 3  
 Andriillat Y., Jaschek M., Jaschek C., 1988, *A&AS*, 72, 129  
 Andriillat A., Jaschek M., Jaschek C., 1990, *A&AS*, 84, 11  
 Aret A., Kraus M., Muratore M. F., Borges Fernandes M., 2012, *MNRAS*, 423, 284  
 Arkhipova V. P., Ikonnikova N. P., 1992, *Sov. Astron. Lett.*, 18, 418  
 Arkhipova V. P., Ikonnikova N. P., Komissarova G. V., Esipov V. F., 2006, *Astron. Lett.*, 32, 594  
 Báez-Rubio A., Martín-Pintado J., Thum C., Planesas P., 2013, *A&A*, 553, A45  
 Báez-Rubio A., Martín-Pintado J., Thum C., Planesas P., Torres-Redondo J., 2014, *A&A*, 571, L4  
 Baines D., Oudmaijer R. D., Porter J. M., Pozzo M., 2006, *MNRAS*, 367, 737  
 Barsukova E. A., Borisov N. V., Burenkov A. N., Goranskii V. P., Klochkova V. G., Metlova N. V., 2006, *Astron. Rep.*, 50, 664  
 Bergner Y. K. et al., 1990, *Astrofizika*, 32, 203  
 Borges Fernandes M., de Araújo F. X., Bastos Pereira C., Codina Landaberry S. J., 2001, *ApJS*, 136, 747  
 Borges Fernandes M., Kraus M., Chesneau O., Domiciano de Souza A., de Araújo F. X., Stee P., Meilland A., 2009, *A&A*, 508, 309  
 Borges Fernandes M. et al., 2011, *A&A*, 528, A20  
 Borges Fernandes M., Kraus M., Nickeler D. H., De Cat P., Lampens P., Pereira C. B., Oksala M. E., 2012, *A&A*, 548, A13  
 Briot D., 1981, *A&A*, 103, 1  
 Carmona A., van den Ancker M. E., Audard M., Henning T., Setiawan J., Rodmann J., 2010, *A&A*, 517, A67  
 Cerrigone L., Hora J. L., Umama G., Triguilio C., 2009, *ApJ*, 703, 585  
 Chengalur J. N., Lewis B. M., Eder J., Terzian Y., 1993, *ApJS*, 89, 189  
 Chentsov E. L., Klochkova V. G., Miroshnichenko A. S., 2010, *Astrophys. Bull.*, 65, 150  
 Cidale L. S., Ringuélet A. E., 1993, *ApJ*, 411, 874  
 Cidale L., Zorec J., Tringaniello L., 2001, *A&A*, 368, 160  
 Cidale L. S. et al., 2012, *A&A*, 548, A72  
 Clark J. S., Steele I. A., Fender R. P., Coe M. J., 1999, *A&A*, 348, 888  
 Cohen M., Biegging J. H., Dreher J. W., Welch W. J., 1985, *ApJ*, 292, 249  
 Danks A. C., Dennefeld M., 1994, *PASP*, 106, 382  
 Downes R. A., Keyes C. D., 1988, *AJ*, 96, 777  
 Ekström S. et al., 2012, *A&A*, 537, A146  
 Frasca A., Miroshnichenko A. S., Rossi C., Friedjung M., Marilli E., Muratorio G., Busà I., 2015, *A&A*, preprint ([arXiv:1510.06158](https://arxiv.org/abs/1510.06158))  
 Geballe T. R., Persson S. E., 1987, *ApJ*, 312, 297  
 Gvaramadze V. V., Menten K. M., 2012, *A&A*, 541, A7  
 Hamann F., 1994, *ApJS*, 93, 485  
 Hamann F., Persson S. E., 1992a, *ApJS*, 82, 247  
 Hamann F., Persson S. E., 1992b, *ApJS*, 82, 285  
 Hartigan P., Edwards S., Pierson R., 2004, *ApJ*, 609, 261  
 Hiltner W. A., 1947, *ApJ*, 105, 212  
 Hofmann K.-H., Balega Y., Ikhsanov N. R., Miroshnichenko A. S., Weigelt G., 2002, *A&A*, 395, 891  
 Humphreys R. M., Davidson K., Grammer S., Kneeland N., Martin J. C., Weis K., Burggraf B., 2013, *ApJ*, 773, 46  
 Humphreys R. M., Weis K., Davidson K., Bomans D. J., Burggraf B., 2014, *ApJ*, 790, 48  
 Hutsemekers D., 1985, *A&AS*, 60, 373  
 Hynes R. I. et al., 2002, *A&A*, 392, 991  
 Ishida M., Morio K., Ueda Y., 2004, *ApJ*, 601, 1088  
 Jaschek C., Jaschek M., Egret D., Andriillat Y., 1988, *A&A*, 192, 285  
 Jaschek C., Andriillat Y., Jaschek M., 1996, *A&AS*, 117, 281  
 Klochkova V. G., Sendzikas E. G., Chentsov E. L., 2015, *Astrophys. Bull.*, 70, 99  
 Klutz M., Swings J. P., 1977, *A&A*, 56, 143  
 Kraus M., Krügel E., Thum C., Geballe T. R., 2000, *A&A*, 362, 158

- Kraus M., Borges Fernandes M., de Araujo F. X., Lamers H. J. G. L. M., 2005, *A&A*, 441, 289
- Kraus M., Borges Fernandes M., de Araujo F. X., 2007, *A&A*, 463, 627
- Kraus M., Borges Fernandes M., de Araujo F. X., 2010, *A&A*, 517, A30
- Kraus M., Oksala M. E., Nickeler D. H., Muratore M. F., Borges Fernandes M., Aret A., Cidale L. S., de Wit W. J., 2013, *A&A*, 549, A28
- Kraus M., Cidale L. S., Arias M. L., Oksala M. E., Borges Fernandes M., 2014, *ApJ*, 780, L10
- Kraus M., Oksala M. E., Cidale L. S., Arias M. L., Torres A. F., Borges Fernandes M., 2015, *ApJ*, 800, L20
- Kwan J., Fischer W., 2011, *MNRAS*, 411, 2383
- Lamers H. J. G. L. M., Zickgraf F.-J., de Winter D., Houziaux L., Zorec J., 1998, *A&A*, 340, 117
- Leinert C., 1986, *A&A*, 155, L6
- Liermann A., Schnurr O., Kraus M., Kreplin A., Arias M. L., Cidale L. S., 2014, *MNRAS*, 443, 947
- Lobel A. et al., 2012, in Drissen L., Rubert C., St-Louis N., Moffat A. F. J., eds, *ASP Conf. Ser. Vol. 465, Proceedings of a Scientific Meeting in Honor of Anthony F. J. Moffat*. Astron. Soc. Pac., San Francisco, p. 358
- Lobel A. et al., 2013, *A&A*, 559, A16
- Mariotti J. M., Chelli A., Sibille F., Foy R., Lena P., Tchountonov G., 1983, *A&A*, 120, 237
- Marston A. P., McCollum B., 2008, *A&A*, 477, 193
- Martín-Pintado J., Bachiller R., Thum C., Walmsley M., 1989, *A&A*, 215, L13
- Martín-Pintado J., Thum C., Planesas P., Báez-Rubio A., 2011, *A&A*, 530, L15
- Meilland A., Kanaan S., Borges Fernandes M., Chesneau O., Millour F., Stee P., Lopez B., 2010, *A&A*, 512, A73
- Merrill P. W., 1927, *ApJ*, 65, 286
- Merrill P. W., Burwell C. G., 1933, *ApJ*, 78, 87
- Merrill P. W., Burwell C. G., 1949, *ApJ*, 110, 387
- Millour F., Meilland A., Chesneau O., Stee P., Kanaan S., Petrov R., Mourard D., Kraus S., 2011, *A&A*, 526, A107
- Miroshnichenko A., Corporon P., 1999, *A&A*, 349, 126
- Miroshnichenko A. S., Fremat Y., Houziaux L., Andriillat Y., Chentsov E. L., Klochkova V. G., 1998, *A&AS*, 131, 469
- Miroshnichenko A. S., Klochkova V. G., Bjorkman K. S., Panchuk V. E., 2002, *A&A*, 390, 627
- Miroshnichenko A. S. et al., 2007, *ApJ*, 671, 828
- Miroshnichenko A. S. et al., 2015, *ApJ*, 809, 129
- Monnier J. D. et al., 2004, *ApJ*, 605, 436
- Muratore M. F., Kraus M., de Wit W. J., 2012a, *Bol. Asociación Argentina Astron.*, 55, 123
- Muratore M. F., de Wit W. J., Kraus M., Aret A., Cidale L. S., Borges Fernandes M., Oudmaijer R. D., Wheelwright H. E., 2012b, in Carciofi A. C., Rivinius T., eds, *ASP Conf. Ser. Vol. 464, Circumstellar Dynamics at High Resolution*. Astron. Soc. Pac., San Francisco, p. 67
- Muratore M. F., Kraus M., Oksala M. E., Arias M. L., Cidale L., Borges Fernandes M., Liermann A., 2015, *AJ*, 149, 13
- Muratorio G., Rossi C., Friedjung M., 2008, *A&A*, 487, 637
- Oksala M. E., Kraus M., Cidale L. S., Muratore M. F., Borges Fernandes M., 2013, *A&A*, 558, A17
- Oudmaijer R. D., Drew J. E., Vink J. S., 2005, *MNRAS*, 364, 725
- Plets H., Waelkens C., Trams N. R., 1995, *A&A*, 293, 363
- Polidan R. S., Peters G. J., 1976, in Slettebak A., ed., *Proc. IAU Symp. 70, Be and Shell Stars*. Reidel, Dordrecht, p. 59
- Richardson N. D. et al., 2016, *MNRAS*, 455, 244
- Robinson E. L., Ivans I. I., Welsh W. F., 2002, *ApJ*, 565, 1169
- Rossi C., Frasca A., Marilli E., Friedjung M., Muratorio G., 2011, in Neiner C., Wade G., Meynet G., Peters G., eds, *Proc. IAU Symp. 272, Active OB stars: structure, evolution, mass loss, and critical limits*. Cambridge Univ. Press, Cambridge, p. 422
- Šlechta M., Škoda P., 2002, *Publ. Astron. Inst. Acad. Sci. Czech Republic*, 90, 1
- Stephenson C. B., 1986, *ApJ*, 300, 779
- Strelitski V., Biegging J. H., Hora J., Smith H. A., Armstrong P., Lagergren K., Walker G., 2013, *ApJ*, 777, 89
- Swings J. P., Andriillat Y., 1981, *A&A*, 103, L3
- Thum C., Martín-Pintado J., Bachiller R., 1992, *A&A*, 256, 507
- Thum C., Matthews H. E., Martín-Pintado J., Serabyn E., Planesas P., Bachiller R., 1994a, *A&A*, 283, 582
- Thum C., Matthews H. E., Harris A. I., Tacconi L. J., Schuster K. F., Martín-Pintado J., 1994b, *A&A*, 288, L25
- Thum C., Strelitski V. S., Martín-Pintado J., Matthews H. E., Smith H. A., 1995, *A&A*, 300, 843
- Thureau N. D. et al., 2009, *MNRAS*, 398, 1309
- Venkata Raman V., Anandarao B. G., 2008, *MNRAS*, 385, 1076
- Wheelwright H. E., Oudmaijer R. D., Goodwin S. P., 2010, *MNRAS*, 401, 1199
- Wheelwright H. E., de Wit W. J., Weigelt G., Oudmaijer R. D., Ilee J. D., 2012, *A&A*, 543, A77
- White R. L., Becker R. H., 1985, *ApJ*, 297, 677
- Wisniewski J. P., Babler B. L., Bjorkman K. S., Kurchakov A. V., Meade M. R., Miroshnichenko A. S., 2006, *PASP*, 118, 820
- Zickgraf F.-J., 2003, *A&A*, 408, 257
- Zickgraf F.-J., Wolf B., Stahl O., Leitherer C., Klare G., 1985, *A&A*, 143, 421

This paper has been typeset from a  $\text{\TeX}/\text{\LaTeX}$  file prepared by the author.